Microfluidic MEMS for Semiconductor Processing

Albert K. Henning, *Member, IEEE,* John S. Fitch, James M. Harris, Edward B. Dehan, Bradford A. Cozad, Lee Christel, Youssof Fathi, Dean A. Hopkins, Jr., Les J. Lilly, Wendell McCulley, Walter A. Weber, and Mark Zdeblick

***Abstract*—The advent of MEMS (microelectromechanical systems) will enable dramatic changes in semiconductor processing. MEMS-based devices offer opportunities to achieve higher performance and functionality, at lower cost, with decreased size and increased reliability.**

In this work, we describe the achievement of several important devices for use in the semiconductor equipment industry. They include a low-flow mass flow controller, a high-precision pressure regulator, and an integrated gas panel. Compared to current technology, the devices are ultra-small in size, thus minimizing dead volumes and gas contact surface areas. With wettable surfaces comprised of ceramic and silicon (or, silicon coated with Si_3N_4 or SiC), they are resistant to corrosion, and generate virtually no particles.

The devices are created from modular components. The science and technology of these components will be detailed. The modules examined are: normally-open proportional valves; normally-closed, low leak-rate shut-off valves; critical orifices (to extract information of flow rate); flow models (to extract flow rate from pressure and temperature information); silicon-based pressure sensors; and, the precision ceramic-based packages which integrate these modules into useful devices for semiconductor processing.

The work finishes with a detailed description of the low-flow mass flow controller.

***Index Terms*—Integrated fluidic systems, mass flow controller, microfluidics, microvalves, vacuum leak rate shut-off valve.**

Nomenclature

dV_F, V_o	Volumetric change and initial volume of fluorinert.
β	Temperature coefficient of expansion of fluorinert liquid.
$T_{\rm FC}, T_{\rm fill}$	Mean and fill temperatures of Fluorinert liquid.
T_R, T_A	Resistor and ambient temperatures.
z	Equilibrium membrane-to-NO-inlet gap.
s	Membrane stroke (departure from equilibrium position).
a	Membrane radius.
h, t	Membrane, cavity thickness.
P	Pressure differential across the membrane.
E, μ	Young's modulus (190 000 MPa) and Poisson's ratio (0.09) for crystalline silicon.
σ	Membrane stress.
$\dot{m}$	Mass flow (typically in cm^3/min, normalized to the STP flow at 273 K [sccm]).
$P_{\rm in}, P_{\rm out}, P_x$	Inlet, outlet, intermediate (pressure sensor) pressures.
ν, K	Flow velocity, loss coefficient.
γ	Ratio of specific heats, c_p/c_v.
α	$\sqrt{\gamma(2/1+\gamma)^{\gamma+1/\gamma-1}}$.
δ	$\sqrt{4\gamma/(\gamma+1)(\gamma-1)}$.
R	Gas constant in $p = \rho RT$ (8314 m^2/K-s^2 divided by mol. wt.).
ρ	Gas density.
D, A, C_d	Diameter, area, and coefficient of discharge for an orifice.

Manuscript received March 22, 1998; revised August 7, 1998. This work was presented in part at the Second IEEE International Conference on Innovative Systems in Silicon, Austin, TX, October 1997. This work was supported in part by DARPA under Contract DAAL-01-94-C-3401.

A. K. Henning, J. M. Harris, E. B. Dehan, B. A. Cozad, D. A. Hopkins, Jr., L. J. Lilly, and W. A. Weber are with Redwood Microsystems, Inc., Menlo Park, CA 94025 USA.

J. S. Fitch was with Redwood Microsystems, Inc., Menlo Park, CA 94025 USA. He is now with Xerox Palo Alto Research Center, Palo Alto, CA 94304 USA.

L. Christel was with Redwood Microsystems, Inc., Menlo Park, CA 94025 USA. He is now with Cepheid, Sunnyvale, CA 94089 USA.

Y. Fathi was with Redwood Microsystems, Inc., Menlo Park, CA 94025 USA. He is now with Maxim Integrated Products, Sunnyvale, CA 94089.

W. McCulley was with Redwood Microsystems, Inc., Menlo Park, CA 94025 USA. He is now with SSI Technologies, Janesville, WI 53547-5011 USA.

M. Zdeblick was with Redwood Microsystems, Inc., Menlo Park, CA 94025 USA. He is now with Stanford University, Stanford, CA 94035 USA.

Publisher Item Identifier S 1070-9894(98)08527-2.

I. Introduction

The present and future requirements of the semiconductor industry for gas distribution and control are well documented [1], [2]. The arrival of facilities to fabricate 300 mm silicon wafers creates opportunities for new technologies to meet the challenging performance, cost, yield, and reliability specifications for devices manufactured in these facilities.

The gas control and distribution portions of these facilities will be faced with particular challenges. Particles must be reduced in size and number. This reduction requires: increased materials compatibility with process gases; decreased dead space volumes; decreased numbers of, or improved welds; and decreased numbers of, or improved, face seals.

Several conventional means to meet these challenges have been proposed [3]. Approaches based on microelectromechanical systems (MEMS) [4] offer numerous advantages. Materials in silicon-based microvalves and microfluidic systems are compatible with a wide range of electronics specialty gases (ESG). Where the gas in question is corrosive to silicon, thin film coatings such as SiC and Si_3N_4 may be used to coat the wetted surfaces and restore corrosion resistance [5]. Decreased dead volumes have already been demonstrated in micro chemical analysis systems [6]. Laboratory versions of MEMS-based electrostatic microvalves have been reported [7].

1070–9894/98$10.00 © 1998 IEEE

In this work, we report the use of our MEMS-based thermopneumatic valve, pressure regulator, and mass flow controller (MFC) technologies [8] to create ultraclean, integrated gas sticks, pressure regulators, shut-off valves, and mass flow controllers for ESG distribution. The use of MEMS components and modules minimizes, or eliminates altogether, the size and number of welds and face seals used in integrated gas control and distribution components. Dead space volumes and wetted surface areas are reduced dramatically. When fabricated using materials compatible with ESG, the generation of particles leading to product defects is also greatly reduced.

This paper first describes the MEMS-based *modules* used as the building blocks for ultraclean gas control and distribution *devices* and *systems*. Following this description, the devices themselves are discussed. Finally, a detailed presentation of one of these devices, a low-flow mass flow controller (for He backside wafer cooling, and for control of low-flow, critical etch and deposition processes) completes our discussion.

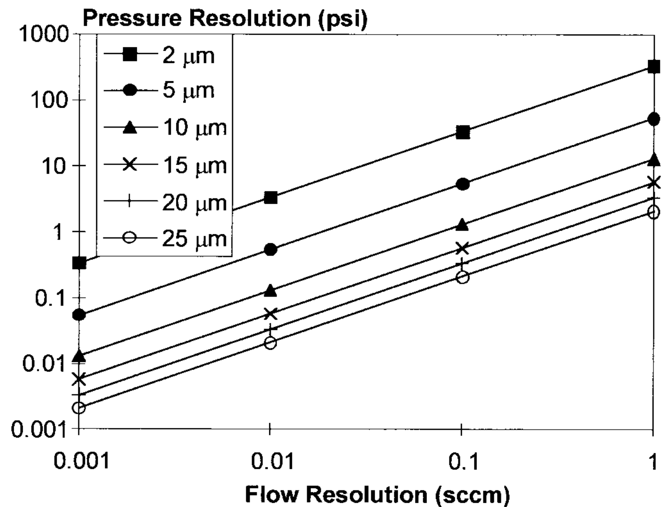

Fig. 1. Pressure sensor resolution required to achieve a given flow resolution, as a function of critical orifice hydraulic diameter.

II. MEMS Modules

In order to create a true system, MEMS-based devices require a number of modules. The modules utilized in our gas control and distribution devices are: the underlying flow model (supported by the electronics); critical flow orifices; normally-open proportional valves; normally-closed, low-leakage shut-off valves; temperature and pressure sensors; and the advanced ceramic packages which enable the combination of modules into higher-level devices and systems.

A. Flow Models

In microelectronics, assembling individual transistors to create devices—such as static random access memories—with higher levels of functionality requires simple models to relate transistor terminal voltages to the flow of electrons or holes. Similarly, in microfluidics, assembling individual components into higher-level devices and systems demands simple models relating nodal pressures to component gas flow. Such models can be derived from compressible gas flow theory, where the flow may be either sonic or subsonic [9]. Consider for a moment the flow of ideal gases through a beveled orifice. The expressions for the flow can then be broken into subsonic and sonic (or choked) flow regimes. The expression for subsonic flow is

$$\dot{m} = \frac{P_{\text{in}}}{\sqrt{RT}} C_d A \left(\frac{P_{\text{out}}}{P_{\text{in}}}\right)^{1/\gamma} \delta(\gamma) \sqrt{\left(\frac{P_{\text{in}}}{P_{\text{out}}}\right)^{(\gamma-1)/\gamma} - 1} \quad (1)$$

while the expression for sonic flow is

$$\dot{m} = P_{\text{in}} C_d A \, \frac{\alpha(\gamma)}{\sqrt{RT}}. \quad (2)$$

Sonic flow (sometimes referred to as 'choked' flow) occurs when the gas flow exceeds the speed of sound for the given conditions of temperature and pressure. In both these equations, the coefficient of discharge C_d does not depend upon pressure or temperature, but depends only upon the structural shape (not size) of the orifice. The orifice area is A. Gas-specific effects are contained in the terms related to R and γ. The effect of temperature T is given explicitly, leaving nodal (inlet and outlet) pressures responsible for the remaining nature of the flow.

Control devices can be created by joining two or more modules or components in either series or parallel combination. In the mass flow controller example described later in this work, an orifice with a variable-size area (that is, a microvalve) is placed in series with a fixed-area orifice. Sonic and subsonic flow equations then describe the flow through the series combination, allowing unique determination of the nodal pressure between the two components as a function of the flow, thus describing completely the system behavior.

Since flow is determined from nodal pressures, such pressures must in practice be measured. In instances where either sonic or subsonic flow is allowed in a flow component modeled as an orifice, two pressure sensors are required on either side of the component (see Fig. 9), in order to extract the measured flow. In many applications, however, the component outlet pressures are on the order of 10–200 Torr, allowing sonic flow to be assumed, and enabling the use of a single pressure sensor. Typically, the inlet pressure must exceed the outlet pressure by a factor of 2, to ensure sonic flow conditions, although this factor is gas-dependent [9].

As mentioned above, a microvalve can be treated as a variable-area orifice. In the case of a normally-open microvalve, this characteristic requires some modification of the flow models described in (1) and (2). These modifications will be discussed in the section below on normally-open valves.

B. Critical Flow Orifices

The critical orifices used in our devices and systems are fabricated using silicon micromachining technology. 'Critical' means that the flow exceeds the sound velocity through the orifice. Conventional, wet anisotropic etching is used to create the sharp, beveled orifices required for (2) to hold.

Flow resolution in, for instance, an MFC is closely tied to the size of the critical orifice. Fig. 1 shows the nature of this relationship, which is derived by differentiation of (2)

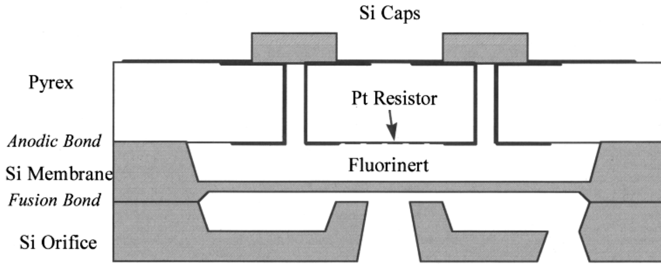

Fig. 2. Cross section schematic of a thermopneumatically-actuated, normally-open, proportional microvalve. The valve inlet (center hole) is typically the smallest of the two holes.

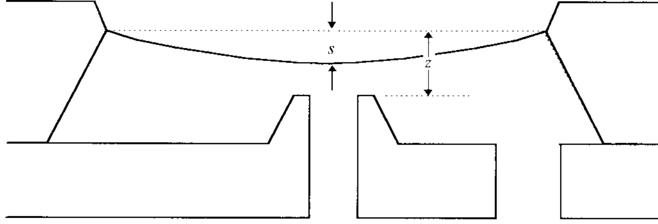

Fig. 3. Relationship between the equilibrium membrane-to-inlet distance z and the stroke s.

with respect to the orifice inlet pressure P_{in}. Helium flow is assumed. For example, if a flow resolution of 0.01 sccm is desired, and the minimum pressure resolution available (from an associated pressure sensor) is 0.03 psia, then the critical orifice's linear dimension must be less than 15 μm.

C. Normally Open Valve

Normally-open (NO) proportional control valves using thermopneumatic actuation have been reported since 1986 [10]. Recently, use of these valves has been extended to include control of liquids, over wide ranges of temperature and pressure [11]. Fig. 2 shows a cross section of an NO proportional control valve. The fabrication process has been described elsewhere [11], but relies on both silicon fusion bonding [12], and silicon-to-Pyrex anodic bonding [13]. Since the valve is surface mounted, no Pyrex is exposed to the fluid traversing the valve. Typical dimensions are: 6.0 $\times$ 6.3 mm^2 lateral dimension; 0.8 mm thick Pyrex; 0.4 mm thick membrane layer, with 50 μm thick membrane; 0.4 mm thick orifice layer; 25–500 μm orifice.

The thermopneumatic actuation principle relies on a hermetically sealed cavity, which is filled with Fluorinert (FC). The cavity incorporates a platinum resistor, to provide controlled heat transfer to the FC liquid. The cavity is rigid on five of its six sides. The sixth side is comprised of a flexible, single-crystal silicon membrane. Heating the FC liquid causes it to expand. The membrane moves in response to this expansion, and ultimately forms a seal with the valve seat, which is also comprised of silicon.

Fig. 3 shows a schematic representation of the membrane deformation, related to the variables in the following equations. The behavior of the NO device is described in [8]. Additional descriptions for the behavior of single-crystal silicon membranes may be found in [14].

For normally-open valves, where the flow through an inlet impinges on the valve membrane, an alternative approach to (1) and (2) is to describe the flow in terms of a loss coefficient K, defined as $K \equiv \Delta P/(\rho_{\text{in}} v^2/2)$. If the mass flux is expressed as $\dot{m} = \rho A v$, then the flow (regardless of sonic or subsonic regime) can be expressed as

$$\dot{m} = A\sqrt{\frac{2}{K}\,\rho_{\text{in}}(P_{\text{in}} - P_{\text{out}})}. \tag{3}$$

In this instance, the expression for our measured loss coefficients, for impingement flow, is

$$\begin{aligned} K = {} & 241.23 \cdot \exp\left(-\frac{(z-s)/D_{\text{inlet}}}{0.027}\right) \\ & + 5.854 \cdot \exp\left(-\frac{(z-s)/D_{\text{inlet}}}{0.546}\right) \end{aligned} \tag{4}$$

where z is the distance between the valve membrane and the valve inlet orifice at full-open flow, and D_{inlet} is the hydraulic diameter of the valve inlet. K modulates, in effect, the orifice-equivalent area A of the microvalve. Equation (4) was determined from a best-fit (double exponential fit) of (3), for a wide variety of measured flows as a function of z-s, P_{in}, and P_{out}. It is valid when $z - s/D_{\text{inlet}}$ is greater than approximately 0.01, since the empirical expression for K does not approach the expected value of infinity as this ratio goes to zero.

In terms of describing the behavior of the microvalve, the following equations provide the most immediate physical insight. Equation (5) describes the change in volume in the sealed cavity, as a function of the coefficient of thermal expansion of the FC liquid, fill temperature of the liquid, and mean temperature of the liquid

$$dV_F = V \times_0 \beta \times (T_{\text{FC}} - T_{\text{fill}}). \tag{5}$$

The change in cavity volume is also related to the geometrical shape of the membrane as it deforms. If the membrane is assumed to be circular

$$dV_F = \frac{1}{6}\,\pi s(3a^2 + s^2) \cong \frac{\pi}{2}\,sa^2. \tag{6a}$$

These expressions create a relationship between the membrane stroke s (the departure from its equilibrium position z), and the power input to the valve as defined by the mean FC temperature T

$$dV_F = \frac{1}{6}\,\pi s(3a^2 + s^2) \cong \frac{\pi}{2}\,sa^2. \tag{6b}$$

Combining (6a) and (6b), and assuming the FC cavity volume $V_0 = \pi a^2 t$, then the stroke s may be expressed as

$$s = 2t\beta(T_{\text{FC}} - T_{\text{fill}}). \tag{6c}$$

Since the system is linear, then in steady-state, and in the absence of convective heat transfer, there is a linear relationship between the mean temperature of the FC liquid, $T_{\text{FC}} \equiv (T_R + T_A)/2$, and the power input to the platinum heater resistor. The constant of proportionality between the input power and the mean FC temperature depends upon the details of the microvalve structural dimensions.

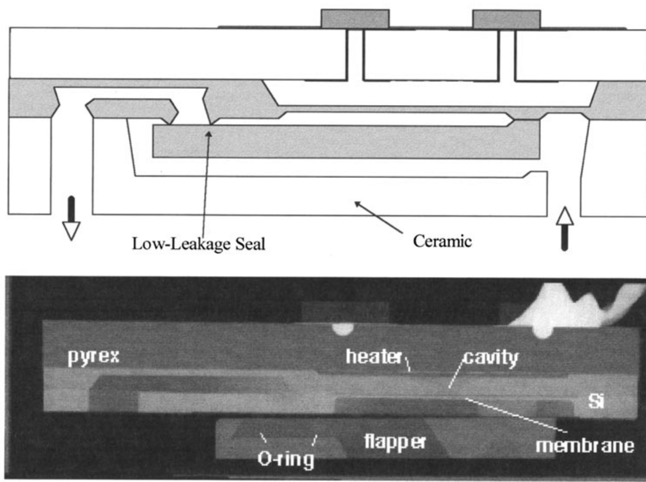

Fig. 4. Top: Cross section schematic of a thermopneumatically-actuated, normally-closed, vacuum leak-rate, shut-off microvalve. Bottom: X-ray tomographic image of an actual valve.

The stroke s may also be considered as a response to P, the transmembrane pressure [14]

$$s = 0.0151 \cdot (1 - \mu^2) \cdot \frac{Pa^4}{Eh^3}. \tag{7}$$

Simultaneously, the deformation of the membrane creates stress in the silicon [14]

$$s = 0.0491 \cdot (1 - \mu^2) \cdot \sigma \cdot \frac{a^2}{Eh}. \tag{8}$$

From a design perspective, then, an NO valve must meet the ambient temperature specifications, while closing against the specified system pressures, while minimizing the power consumption, and staying well below the fracture strength of the crystalline silicon.

D. Normally Closed Shut-off Valve

Normally-closed (NC) valves are important components of other MEMS-based microvalve devices [15]. We report here the development of NC valves which have a wetted path which is entirely ceramic (Al_2O_3) or silicon. These valves also have incorporated a proprietary sealing technology, which enables very low leak rates to be obtained [16]. As with the NO valve modules, wetted surfaces may be coated with SiC or Si_3N_4, in order to provide materials compatibility in situations where a wetted silicon surface would be undesirable.

Fig. 4 shows both schematic and actual cross sections of this normally-closed, low-leakage shut-off valve. The actual image was obtained using x-ray tomographic techniques. The thermopneumatic actuation principle is still employed. In this case, however, a boss is added to the silicon membrane, and a silicon cantilever is fusion-bonded to the boss. Under conditions of zero input power, this cantilever will provide the shut-off property by sealing against a low-leakage seat. As shown, the wetted path is entirely silicon or ESG-compatible ceramic. The silicon-ceramic interface is a eutectic bond. The overall dimensions are 8 mm × 6 mm × 2 mm, and are (roughly) to scale.

SEMATECH has established specifications for shut-off valves, which state that the leak rate must be 10^{-9} cc-He/s or less when measured 15 s after application of the signal to shut-off. Fig. 5 shows measured helium leak rates for a set of microvalves. The sealing material in these devices is Viton. We are in the process of characterizing seals made with other materials, such as Kel-F. Also shown is data from a standard shut-off valve commonly used in the industry. The background leak rate of the test fixture itself is also given, and provides a baseline for all of the measurements. As shown, normally-closed shut-off microvalves can achieve the same leak rate standards of conventional shut-off valves.

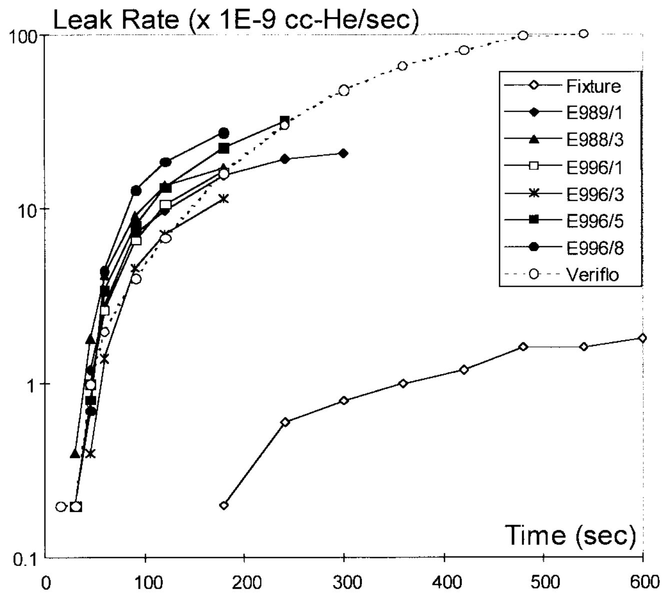

Fig. 5. Helium leak rate measurements for vacuum leak-rate shut-off microvalves.

It is interesting to compare the steady-state leak rate of the microvalves, and that of conventional valves. Shut-off valves used at present in the industry reach much higher steady-state helium leak rates (approximately 200 × 10^{-9} atm-cc/s) than our microvalves. Conventional valves have larger effective areas for leaking gas, use more permeable sealing materials, and have smaller compression forces on the sealing surfaces. On the other hand, the length of the leak path for conventional shut-off valves is greater than in the microvalve, resulting in occasionally lower metastable (or transient) values of leak rate.

E. Sensors (Pressure, Temperature)

In our present devices, small (several millimeters square) silicon temperature sensors and piezoresistive silicon pressure sensors are used to monitor temperature and pressure in the device flow path. These sensors are available commercially. When incorporated into a final flow control device, the information they provide becomes the basis for the temperature and pressure calibration data which is stored on E^2PROM. It is important that sensing occur as close as possible to the flow point of interest. For instance, in a low-flow MFC, the pressure must be sensed as close as possible to the inlet of the critical orifice.

Thermally induced package stress plays a large role in the long-term behavior of these sensors, especially the pressure

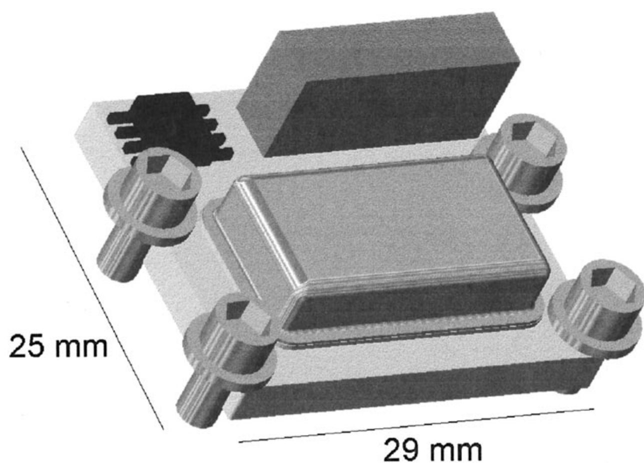

Fig. 6. Example isometric view of a pressure regulator, MFC, or shut-off valve. In, for instance, an MFC, the metal cap (lower center) provides encapsulation of the temperature and pressure sensors, and the normally-open microvalve. The E^2PROM (upper left) contains calibration information for the critical flow orifice. Electrical connections for command and monitor of the MFC are shown in the upper right.

sensors. In order to meet the specifications for a given device, care must be taken in the choice of sensor type, size, shape, placement on the package, and die attach material. Long-term drift of sensor behavior can be explored using accelerated life-test techniques. Such techniques include application of high and low temperatures, application of high and low ambient pressures, and application of mechanical stress to the device package.

F. Advanced Ceramic Packaging

Ceramics available as a result of advances in semiconductor integrated circuits have the structural and materials properties required for application to ESG delivery and control. Fig. 6 extends the cross section of Fig. 3, and shows an isometric view of the use of such ceramics for pressure regulation, mass flow control, or low-leakage shut-off applications. An E^2PROM, which holds the calibration constants for the particular device, as well as constants for a variety of gases, is easily integrated with the ceramic. A metal lid provides a hermetic seal for the valve modules, and the pressure and temperature sensing modules. Electronic control signals are communicated via metal lines patterned on the ceramic surface.

III. Gas Distribution Devices and Systems

These MEMS-based modules can be combined to create a hierarchy of gas control and distribution devices. Some of these devices, such as the pressure regulator or the MFC, can themselves be used to build systems with still higher levels of functionality, in the form of, for instance, a fully integrated, multiple-channel gas panel.

Fig. 7 shows the schematic and isometric views of a fully-integrated gas panel, comprised of four single-channel gas sticks. The manifold on which the individual modules reside is typically built from stainless steel. The size of this gas panel compares very favorably to existing designs. As shown in Fig. 8 and Table I, our 1997 panels, with identical functionality, occupy one-tenth the internal volume of 1996 panel designs, and one-half the length (one-fourth the area) of 1996 designs.

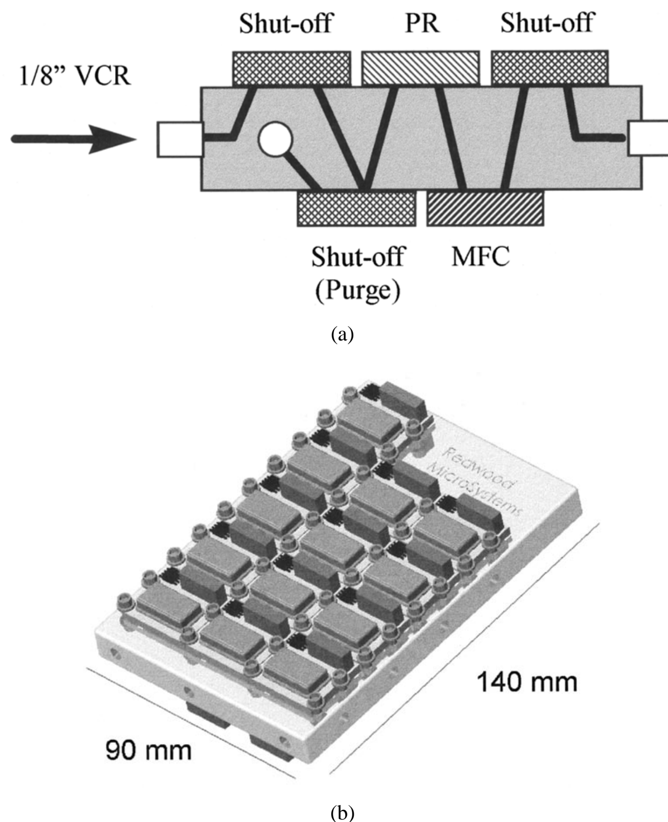

Fig. 7. (a) Schematic of the integrated gas stick. (b) Isometric view of a four-channel gas stick.

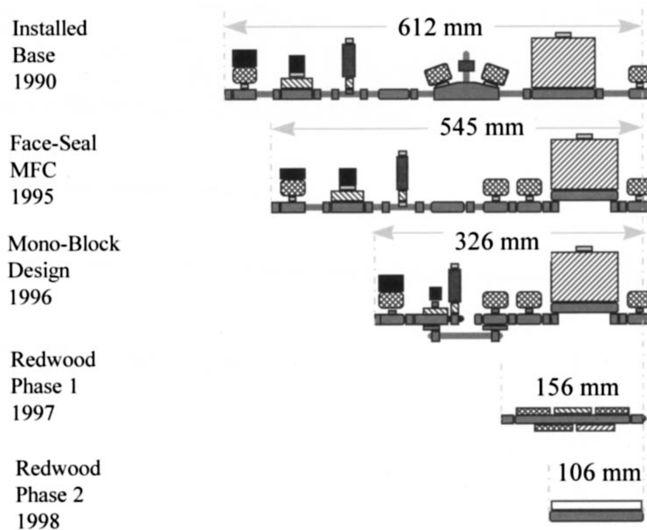

Fig. 8. Size comparison of present and future integrated gas sticks/panels (after [3]).

IV. Low-Flow Mass Flow Controller

As an example of an integrated flow distribution and control device, we will focus upon a low-flow mass flow controller. Fig. 9 shows a schematic of this device, which uses pressure-based flow sensing as described in this work. Table II gives

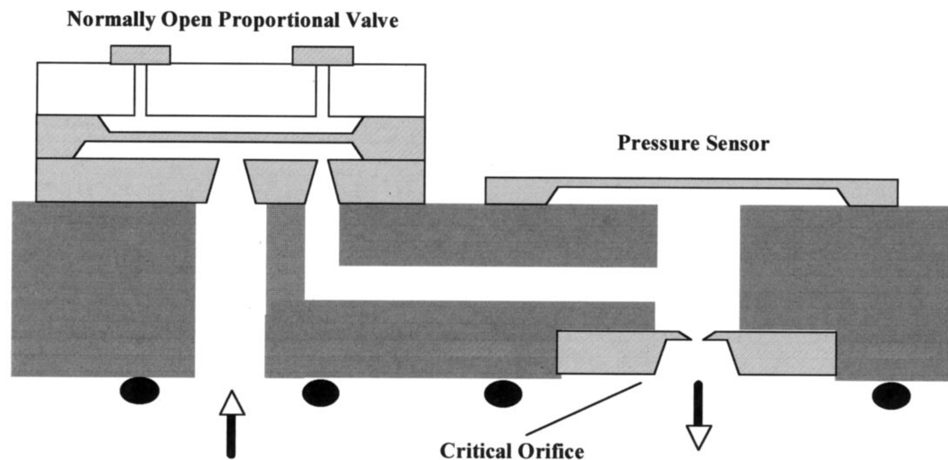

Fig. 9. Schematic representation of the low-flow mass-flow controller. The silicon components are attached to the ceramic substrate using an appropriate polymer-based die attach material, or via eutectic bonding. The encapsulation lid (see Fig. 6), which is not shown here, maintains the vacuum reference pressure for the differential pressure sensor.

TABLE I
FUNCTIONAL COMPARISON OF PRESENT AND FUTURE INTEGRATED GAS STICKS/PANELS (AFTER [3])

	# of Welds	# of Seals	Internal Volume
1990	10	0	38 cc
1995	6	8	31 cc
1996	3	12	22 cc
1997	0	10	2 cc
1998	0	0	<1 cc

TABLE II
SPECIFICATION FOR PRESSURE-BASED MFCS

Fluid Media:	Corrosive and Non-Corrosive Gases and Liquids
Maximum Flow Rates:	1, 2, 5, 10, 20, 50, 100, 200, 500, 1000 sccm
Turndown Ratio:	5:1
Accuracy:	± 1% of full-scale
Repeatability:	± 0.1% of full-scale
Resolution:	0.05% of full-scale
Response Time:	500 ms typical
Leak Rate:	5 x 10^{-6} cc/sec He
Inlet Pressure Range:	25 to 50 psig
Maximum Outlet Pressure:	10 Torr
Ambient Temperature Range:	0 to 50°C
Power Consumption:	3.5 W typical
Dimensions:	106 mm x 40 mm x 25 mm

a sample specification. The flow range and resolution is set by the critical orifice, as depicted in Fig. 1. 'Turndown ratio' defines the flow range over which the stated specifications are met in full.

A. Principles of Operation

Using the flow models of (1) and (2), it is possible to model the steady-state behavior of the low-flow MFC. A series combination of a critical orifice (CO) and normally-open valve (NO) is the simplest device-level flow model, as shown in Fig. 10. The CO is defined by (1) and (2). Using a more

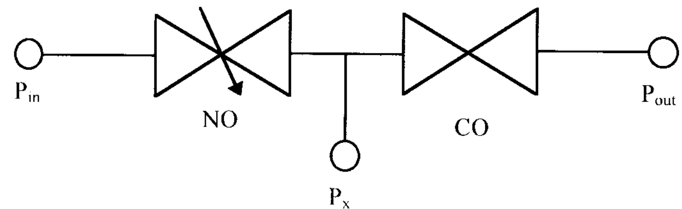

Fig. 10. Schematic representation of the compressible flow model for the series combination of a normally-open proportional valve, and a critical orifice.

simplistic approach than that given in (3) and (4), the NO microvalve flow may also be defined by (1) and (2), provided the orifice-effective flow area is taken to be the wall of a cylindrical tube which varies in area

$$A_{\mathrm{NO}} = \pi D_{\mathrm{NO}}(z - s) \tag{8}$$

P_x represents the pressure to be sensed by the pressure sensor, which will be fed back into the electronics in order to control the NO valve. As opposed to the models of (3) and (4), this simple flow model assumes isentropic flow of a compressible gas. That is, no losses via friction or work (momentum changes) are considered.

Fig. 11 shows an example of the output of the flow model. "0% Power" is taken to be the full-open flow state of the NO valve; correspondingly, "100% Power" would be commensurate with the valve fully shut off, with the membrane seated firmly over the inlet. Fig. 12 shows the measurements from a completed MFC, compared to modeled behavior. In Fig. 11, the intersection of the NO and CO flow curves determines the value of the pressure P_x, as a function of the membrane-to-inlet gap $z - s$. Using (2), this pressure also determines the mass flow. When the NO valve is unpowered, the membrane-to-inlet gap is the full value z, and very little pressure is dropped across the NO valve. As s increases, more pressure is dropped across the NO, and the flow decreases. Power input to the NO valve is responsible for increasing s, as shown in (6), and decreasing the membrane-to-inlet gap.

The control electronics manage the relationship between pressure and temperature sensors, and power input to the NO microvalve. The sensors—which reside near the critical orifice,

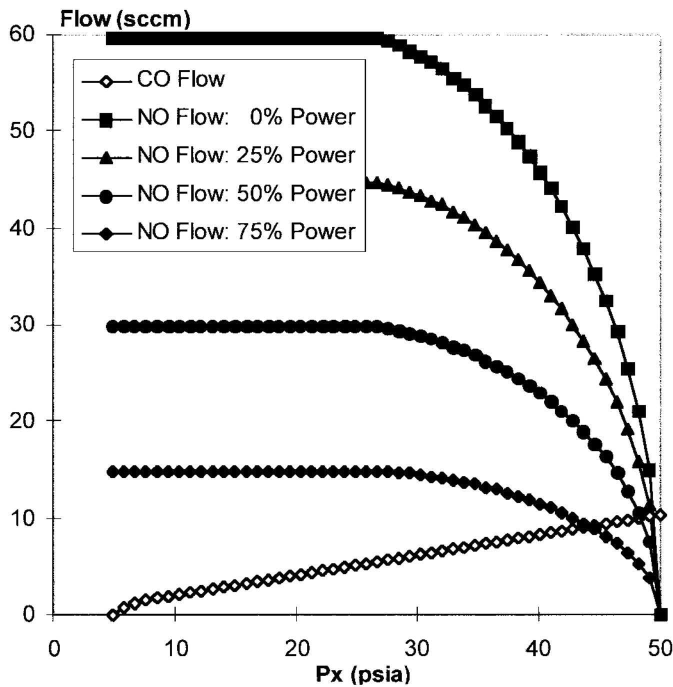

Fig. 11. Example of the compressible flow model for a 10 sccm MFC. The open diamonds describe the critical flow orifice, while the filled symbols describe the NO valve, for various values of input power (corresponding to the position of the membrane relative to the NO valve inlet). The intersection of a valve curve and the critical flow orifice curve determines uniquely the value of P_x and mass flow.

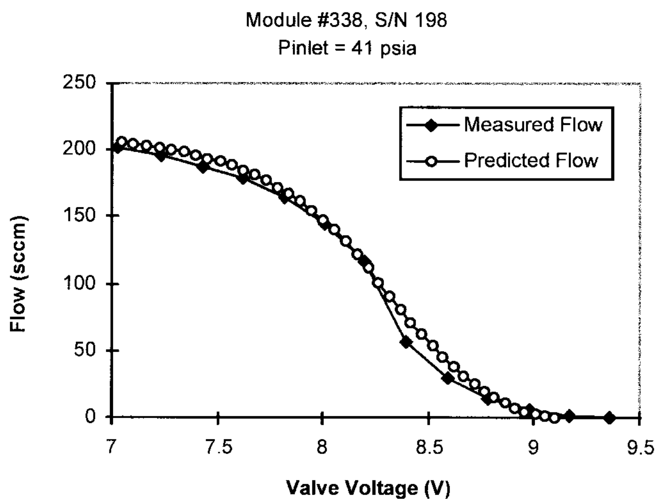

Fig. 12. Comparison of measurements and modeling of the flow versus valve voltage characteristics for a 200 sccm MFC.

and which have been calibrated and characterized prior to placing the MFC into service—are used with (2) to extract the mass flow rate. Control of the mass flow is effected by comparing the extracted flow to the set point flow. If the extracted flow is too high compared to the set point, additional power is sent to the NO valve, increasing s, and decreasing the MFC flow. If the extracted flow is too low, the power input to the NO valve is decreased, causing $z - s$ to decrease back toward the unpowered value z. Temperature-dependent information, compensating for temperature-induced package stresses on the pressure sensor, and temperature-related changes in flow in (2), are stored in an E^2PROM on the MFC module (see Fig. 6).

V. Discussion

Variations in device performance are expected, as a function of variations in valve and orifice structural sizes and shapes imposed by the required microfabrication techniques. From a modeling perspective, such variations may be discerned by the interested reader from the modeling equations given. Provision of details here, however, lies beyond the scope of the present work, and will be discussed elsewhere. Experimental variations can, however, be seen in Fig. 5, for the shut-off valve. We have observed similar valve-to-valve variations in normally-open valves.

Since our microvalves are *thermal devices*, it is the input *power* which controls the flow, not the input voltage. Control voltage is set by adjusting the resistance of the Pt heater resistor, with foreknowledge of the power required to control the valve.

Due to issues of yield and market acceptance, it is not at present viable nor desirable to increase the level of integration and miniaturization of the high-level devices or systems reported here. Clearly, however, they are amenable to considerable further reductions in size, should circumstances change in the future.

Valve response time is principally a function of input power, and thermal resistance between the valve and the package. As a thermal device, however, sub-millisecond valve response times are intrinsically unlikely without significant scaling down of valve size.

The primary barriers for further development of devices and systems based on microfabricated valves do not derive from the microvalves themselves, but rather from the pressure and temperature sensors used to create them. For instance, thermal-induced stresses affect the long-term drift of the sensors, and so the accuracy of, say, an MFC over long periods of time.

VI. Conclusion

We have demonstrated the science and technology required to design and fabricate flow distribution and control devices suitable for the semiconductor processing industry. Components such as pressure-based flow models, critical orifices, pressure and temperature sensors, normally-open proportional valves, and normally-closed vacuum leak rate shut-off valves, have been developed. The valve actuation is based on previously developed thermopneumatic techniques. These components have been integrated into shut-off valve, mass flow controller, and pressure regulator modules, which themselves are combined at a higher level into integrated gas panels. Each integrated device has the benefit of small size, lower cost, higher resolution, materials compatibility, and lowered defect generation, which are among the attributes of the successful application of MEMS-based technology.

Acknowledgment

The authors would like to thank M. Barrera, D. King, and B. Kozen, whose efforts have been crucial in the development of the devices described in this work, R. Abad, E. Falsken, G. Helstrom, K. Hirano, Y. Hua, A. Moreno, and K. Sterritt whose efforts are also gratefully acknowledged, and J. Leu and

A.-M. Lanzillotto, David Sarnoff Research Labs, for obtaining the x-ray tomographic pictures of the vacuum leak-rate shut-off valve

REFERENCES

[1] *The National Technology Roadmap for Semiconductors*, Semiconductor Industry Association, San Jose, CA, 1994.

[2] See, for instance, various papers presented in the *43rd Nat. Symp. Amer. Vacuum Soc., Manufact. Sci. Technol. Tech. Group*, Philadelphia, PA, Oct. 14–18, 1996.

[3] J. Cestari, D. Laureta, and H. Itafuji, "The next step in process gas delivery: A fully integrated system," *Semiconduct. Int.*, pp. 79–87, Jan. 1997.

[4] P. W. Barth, "Silicon microvalves for gas flow control," in *Proc. Transducers Int. Conf. Solid State Sens. Act.*, 1995, pp. 276–279.

[5] A. F. Flannery, N. J. Mourlas, C. W. Storment, S. Tsai, S. H. Tan, and G. T. A. Kovacs, "PECVD silicon carbide for micromachined transducers," in *Proc. Transducers Int. Conf. Solid State Sens. Act.*, 1997, pp. 217–221.

[6] S. Shoji, B. Van der Schoot, N. de Rooij, and M. Esashi, "Smallest dead volume microvalves for integrated chemical analyzing systems," in *Proc. Transducers Int. Conf. Solid State Sens. Act.*, 1991, pp. 1052–5.

[7] M. Esashi, S. Eoh, T. Matsuo, and S. Choi, "The fabrication of integrated mass flow controllers," in *Proc. Transducers Int. Conf. Solid State Sens. Act.*, 1987, pp. 830–833; J. Robertson, "An electrostatically-actuated integrated microflow controller," Ph.D. dissertation, Univ. Michigan, Ann Arbor, 1996.

[8] M. Zdeblick, "A planar process for an electric-to-fluidic valve," Ph.D. dissertation, Stanford University, Stanford, CA, June, 1988; M. Zdeblick, "Integrated, microminiature electric-to-fluidic valve and pressure/flow regulator," U.S. Patent 4 821 997, 1989.

[9] F. M. White, *Fluid Mechanics*. New York: McGraw-Hill, 1979.

[10] M. J. Zdeblick and J. B. Angell, "A microminiature electric-to-fluidic valve," in *Proc. Transducers Int. Conf. Solid State Sens. Act.*, 1987, pp. 827–830.

[11] A. K. Henning, J. Fitch, E. Falsken, D. Hopkins, L. Lilly, R. Faeth, and M. Zdeblick, "A thermopneumatically actuated microvalve for liquid expansion and proportional control," in *Proc. Transducers Int. Conf. Solid State Sens. Act.*, 1997, pp. 825–828.

[12] P. W. Barth, "Silicon fusion bonding for fabrication of sensors, actuators and microstructures," *Sens. Actuator*, vol. 23, pp. 919–926, 1990.

[13] G. Wallis and D. I. Pomerantz, "Field-assisted glass-metal sealing," *J. Appl. Phys.*, vol. 40, pp. 3946–3949, 1969.

[14] M. di Giovanni, *Flat and Corrugated Diaphragm Design Handbook*. New York: Marcel Dekker, 1982.

[15] See the Fluistor product literature and specifications from Redwood Microsystems (available at http://www.redwoodmicro.com).

[16] Patent applications in process.

Albert K. Henning (M'79) received the A.B. (magna cum laude) and A.M. degrees in physics from Dartmouth College, Hanover, NH, in 1977 and 1979, respectively, and the Ph.D. degree in electrical engineering from Stanford University, Stanford, CA, in 1987.

From 1979 to 1982, he was a Device Physicist with Intel Corporation, Santa Clara, CA, working on device and process development for SRAM and microprocessor applications. From 1982 to 1987, he was a Research Assistant at Stanford University. From 1987 to 1993, he was Assistant Professor of Engineering Science at Dartmouth College. He designed, built, and equipped a Class 100/1000 clean room facility for microelectronics and microstructures teaching and research. He was promoted to Associate Professor in 1993. He spent portions of the 1993–1994 academic year on sabbatical, as a Visiting Scientist in the Microstructures Technology Laboratory, Massachusetts Institute of Technology, Cambridge. In 1996, he joined Redwood Microsystems, Menlo Park, CA, initially as Program Manager (responsible for microvalve MEMS development in the areas of refrigeration and air conditioning, and high-precision mass-flow control), later as Wafer Fab Manager (responsible for all valve microfabrication, microengineering, and manufacturing), and presently as Director of Technology. He received an Analog Devices Career Development Professorship in 1987 and a U.S. patent (on the thermocouple MOSFET) in 1993. He has published over 50 journal and proceedings articles.

Dr. Henning received an IBM Faculty Development Award in 1990 and is a member of Sigma Xi and ASEE.

John S. Fitch received the B.S. degree in mechanical engineering from Northeastern University, Boston, MA, in 1984, and the M.S. degree in mechanical engineering from the University of California at Berkeley, in 1986.

In 1986, he joined Digital Equipment Corporation to work on multichip packaging. In 1989, he joined Digital's Western Research Laboratory and worked on packaging for powerful microprocessors, plastic packaging, heat transfer, and manufacturing processes. From 1995 to 1998, he worked in the MEMS field with Redwood Microsystems, Menlo Park, CA. Silicon microvalves, and their related systems, such as mass flow controllers, were the focus of his work. As a Member of the Research Staff at Xerox PARC, Palo Alto, CA. He is currently involved with design, analysis, and experimentation of novel printing techniques. He has been an Associate Editor of the IEEE TRANSACTONS ON COMPONENTS, PACKAGING, AND MANUFACTURING TECHNOLOGY—PART A, for four years.

Mr. Fitch has organized conferences, such as ITHERM, and has shared the "Best Paper" award from ECTC.

James M. Harris received the Ph.D. degree in materials science from the Massachusetts Institute of Technology, Cambridge.

He has been President and CEO of Redwood Microsystems, Menlo Park, CA, since 1996. He previously was CEO at Akashic Memories and Purus. His background also includes work at IBM and National Semiconductor. He has been granted nine patents and has published six articles.

Edward B. Dehan received the A.B. degree in economics from Dartmouth College, Hanover, NH, and the M.B.A. degree from the Graduate School of Business, Stanford University, Stanford, CA.

He is Vice President of Business Development at Redwood Microsystems, Menlo Park, CA, where he has spent six years identifying and qualifying applications for MEMS valves and MEMS-based fluid control systems.

Bradford A. Cozad received the B.S. degree in physics from the California Polytechnic State University, San Luis Obispo.

From 1977 to 1988, he was a Senior Mechanical Engineer for the Rantec Division of Emerson Electric, Los Osos, CA, responsible for packaging and circuit board design related to high voltage power supples. From 1988 to 1989, he was a Senior Mechanical Engineer with Teledyne, Santa Clara, CA, responsible for several airborne and military TWTA power supplies. From 1989 to 1993, he was Mechanical Engineering Manager of the Power Supply Division, M-Square Microtek, Fremont, CA. In 1993, he joined Redwood Microsystems, Menlo Park, CA, as a Senior Mechanical Engineer. He is responsible for all aspects of the design and development of thermopneumatic microvalves for high vacuum shut-off applications.

Lee Christel received the B.S. degree in applied mathematics and physics from the University of Wisconsin, Madison, and the Ph.D. degree in applied physics from Stanford University, Stanford, CA, in 1981.

From 1982 through 1987, he was Principal Investigator and Project Manager on Contracts from Sandia National Laboratories and the NASA-Jet Propulsion Laboratories to investigate the fabrication of radiation-resistant, ultra-thin silicon solar cells for space applications. This work involved the use of dielectric isolation accomplished with silicon/glass bonding and micromachining techniques. In 1988, he joined NovaSensor, Fremont, CA, where he was a Senior Process Engineer and Manager of the Technology Development. He developed several micromachined silicon products, including a 1 mm pressure sensor, piezoresistive accelerometers for air bag and suspension system applications, and high volume microwave detectors. He was responsible for wafer fabrication process engineering, assembly, laser trim and test development for these products, and coordinated their transfer to production. In 1993, he joined Redwood Microsystems, Menlo Park, CA, where he became Vice President of Product Engineering. He was responsible for design, product, and process development, and release to production of pneumatic pressure and flow regulator products, using micromachined silicon valve components integrated with sensors and microcontroller electronics. He joined Cepheid, Sunnyvale, CA, as a Member of the Founding Team and Director of MEMS Engineering in May, 1997. His primary work has been the development of novel micromachined structures for biological applications, including DNA capture technology for use in PCR-based DNA analysis tools. He has published numerous articles, is the holder of one U.S. patent, and is a co-author on several patents pending.

Youssof Fathi, photograph and biography not available at the time of publication.

Dean A. Hopkins, Jr. received the B.S.E.E. degree in electronics engineering from the California State Polytechnic University, Pomona.

From 1978 to 1980, he was a Process Engineer with United Detector Technology, Hawthorne, CA. From 1980 to 1983, was a Senior Process Engineer with the Opto Materials Group, National Semiconductor, Hawthorne, CA. From 1983 to 1985, he was a Senior Process Engineer with Precision Monolithics, Santa Clara, CA. From 1985 to 1991, he was Chief Process Engineer for IC Sensors, Milpitas, CA. From 1991 to 1995, he held Senior Process Engineering positions with Silicon Microstructures, Fremont, CA, Sentir Semiconductor, Santa Clara, CA, and Microflow, Dublin, CA. In 1995, he joined Redwood Microsystems, Menlo Park, CA, as a Senior Process Engineer, where he is responsible for all aspects of bulk silicon microfabrication processing, for both manufacturing, and research and development.

Les J. Lilly is a Senior Process Engineer for Redwood Microsystems, Menlo Park, CA, responsible primarily for fusion and anodic bonding, and metrology. He has maintained additional duties in the areas of quality control, quality assurance, and failure analysis since he joined Redwood in 1995. He has also served as Wafer Fabrication Supervisor and Manager with Redwood Microsystems, Site Microcontamination Control Engineer for Silicon Systems, Santa Cruz, CA, and Site Contamination Control Specialist for National Semiconductor, Puyallup, WA. During his career, he has held positions in device physics and reliability for Intel, Motorola, United Technologies/Mostek, and NCR.

Mr. Lilly is a senior member of the Institute of Environmental Sciences and a member of the American Chemical Society.

Wendell McCulley is a Senior Scientist at SSI Technologies Inc., Janesville, WI, and is engaged in chip design, development, and package design of their new pressure sensor product line. He has worked in the design and process development of MEMS since 1983. His work at Motorola included development of the first commercially available monolithic integrated pressure sensor. At Honeywell SSED, he worked in improvement of sensor stability, and designed a family of jet engine pressure sensors. As Design Manager at Silicon MicroStructures, he designed their consumer pressure sensor line, performed an NSF phase I study on resonant accelerometers, and developed their early foundry relationship with EXAR which eventually purchased SMI. As part of the DARPA development at Lucas NovaSensor, he contributed to the early development of deep reactive ion etching (DRIE), developed a unique double spring mass accelerometer, and was involved in the early demonstration of the IEEE-1451 smart sensor interface. As President of Tesseract Engineering Consultants, he engaged in various MEMS design and development including pressure, acceleration, micro-relays, and micro-valves. As Staff Scientist at Redwood MicroSystems, Menlo Park, CA, he aided in optimization of existing designs through detailed thermal and mechanical finite element analysis, and contributed to development of the next generation process, and packaging.

Walter A. Weber received the B.S. degree in industrial chemistry from Technikum Winterthur, Switzerland.

He has worked in the areas of thick film manufacturing, MCM (hybrid) assembly, pressure sensor assembly, and electronic packaging design. He has been with Redwood Microsystems, Menlo Park, CA, since 1991.

Mark Zdeblick (M'98) received the B.S. degree in civil engineering and the B.A. in architecture from the University of Illinois at Urbana-Champaign in 1982 and the M.S. degree in aeronautics and astronautics and the Ph.D. degree in electrical engineering from Stanford University, Stanford, CA, in 1984 and 1988, respectively.

In 1989, he founded Redwood Microsystems, Menlo Park, CA. From 1990 through 1996, he served as Chief Technical Officer and Director of Redwood. The company develops microfluidic devices, such as those described in this work, based on the Fluistor technology created through his Ph.D. studies. He was involved in every aspect of the company, including securing financing, developing technology, and managing technology development, and serving as Principal Investigator on Federal research and development contracts. He continues to serve on the Board of Directors for the company. In 1997, he was a Consulting Professor with the Department of Ophthalmology, Stanford University, where he explored the development of microfabricated devices for the control of intraocular pressure in glaucoma patients. In 1998, he founded Aspire Technology, Portola Valley, CA. He serves as President of the company, which develops microfabricated devices for environmental analysis, biotechnology, and medical applications. He holds 12 U.S. and foreign patents, and has published numerous articles on MEMS devices and technology. He is an Associate Editor of *Sensors and Materials Journal*.

Dr. Zdeblick is a member of Tau Beta Pi and Phi Eta Sigma.